399

Analysis and active control for wind induced vibration of beam with ACLD patch

Jinqiang Li[*1,2] and Yoshihiro Narita[2]

[1]*College of Mechanics, Taiyuan University of Technology, China*
[2]*Faculty of Engineering, Hokkaido University, Japan*

Abstract. The structural vibration suppression with active constrained layer damping (ACLD) was widely studied recently. However, the literature seldom concerned with the vibration control on flow-induced vibration using active constrained layer. In this paper the wind induced vibration of cantilevered beam is analyzed and suppressed by using random theory together with a velocity feedback control strategy. The piezoelectric material and frequency dependent viscoelastic layer are used to achieve effective active damping in the vibration control. The transverse displacement and velocity in time and frequency domains, as well as the power spectral density and the mean-square value of the transverse displacement and velocity, are formulated under wind pressure at variable control gain. It is observed from the numerical results that the wind induced vibration can be significantly suppressed by using a small outside active voltage on the constrained layer.

Keywords: wind induced vibration; active control; fluctuating wind; cantilevered beam; velocity feedback

1. Introduction

In the nature, wind widely acts as external random excitations on dynamic systems. The study for suppression of wind-induced vibration has therefore received considerable attention, and up to the present time many literature in this research topic have been published. Using the passive and active tuned mass damper systems, Kwok and Samali (1995) studied the suppression of dynamic response in tall buildings and other structures against wind pressure. Kubo *et al*. (1996) studied the problem to suppress aerodynamic response of square-section tall structures by a moving surface boundary-layer control, and investigated the effective and economical arrangements of rotors. By considering the model parameters and the model error as deterministic, Solari (1997) evaluated the wind-excited response of structures and provided closed form expressions of the first and second statistical moments of the maximum response. Considering the vibration in both along-wind and across-wind directions, Chai and Feng (1997) designed the passive and hybrid mega-sub control systems and examined the performance in tall controlled buildings, and a new tall building model and a more realistic wind load model were employed in their study. Zhang and Roschke (1999) studied the vibration control of a flexible laboratory structure excited by simulated wind forces,

---

∗Corresponding author, Manager, E-mail: lijinqiang@yahoo.com

and minimized along-wind accelerations of vibration by using a LQG/LTR control strategy. Li (2012) employed Hamilton's principle and presented a Rayleigh–Ritz formulation to study active aeroelastic flutter suppression for supersonic plates. Using a layerwise optimization method, Li and Narita (2013) investigated the optimal design problem for supersonic laminated plate. From their numerical results, it is found that taking the fiber orientation angles as design variables one can largely raise the critical aerodynamic pressure and significantly improve the stability of supersonic laminated plates.

The active control of vibration for beam structures has received considerable attention, and many researchers have employed the smart materials in the vibration suppression of beam. Using the spectral finite element method, Lee and Kim (2001) investigated the active vibration control of a beam with ACLD treatment. Balamurugan and Narayanan (2002) provided a beam finite element model to assess the performance of vibration control for beams with covered smart constrained layer. A new model for beams with ACLD patches was developed by Sun and Tong (2004), and in their study both the compressional vibration and shear damping were considered. Using a partial layerwise theory, Vasques *et al*. (2006) developed an one-dimensional finite element model to study the analytical formulation and finite element modelling of beams with ACLD treatments.

Sun and Tong also gave a solution scheme to obtain the eigenvalues and frequency response of the closed-loop controlled beam. Using the energy approach and the Lagrange equation, Cai *et al*. (2006) derived the motion equation for the vibration problem of a beam/ACLD system. Li *et al*. (2008) studied the active vibration control of beams with the active constrained layer damping treatment using Hamilton's principle and the Rayleigh–Ritz method. They derived the equation of motion for the beam-ACLD system and analyzed their numerical results. Lee (2005) studied the vibration and acoustic control of beams with ACLD treatment and obtained the control input that maximizes the loss factor of the ACLD.

Beams are widely used in the structures and buildings, and many structures can be simplified as a beam, and many of these structures are often exposed to wind pressure which may cause serious damages. However, the active control problem of beam structure for wind induced random vibration has seldom been investigated. Based on these technical needs and our previous studies on active vibration control of shell Li and Narita (2012a), in this study an active control method is expanded to reduce wind induced vibration. In the formulation, a Ritz solution is derived by the Hamilton's principle. The active damping and random vibration suppressions are studied by a negative velocity feedback control strategy. The power spectral density and mean-squares displacement and velocity curves are presented to demonstrate the effectiveness of the method.

2. The fluctuating wind pressure

The wind speed profile along the vertical direction of a building is expressed as

$$v(H,t) = v_a(H) + v_d(H,t) \tag{1}$$

where $v_a(H)$ is the mean wind speed which is only related with height H and it is generally considered as a constant. $v_d(H, t)$ is the fluctuating wind speed which is stochastic and changes with time variation, and the fluctuating wind speed could be described by its power spectrum which reflects the energy distribution with frequency.

The pressure that the wind produces on a body in the along-wind direction is of the following form

$$P = \frac{1}{2}C_p\rho_a v^2 \tag{2}$$

where ρ_a is the density of the air (assumed to be 1.225 kg/m^3), C_p is the drag coefficient and in the present paper the drag coefficient is taken to be 1.48 (Kolousek *et al.* 1984).

Substituting Eq. (1) into Eq. (2) and ignoring the small term v_d^2 (v_a is much larger than v_d), the wind pressure can be expressed by $P = P_a + P_d$ while

$$P_a = \frac{1}{2}C_p\rho_a v_a^2 \tag{3}$$

$$P_d = C_p\rho_a v_a v_d \tag{4}$$

where P_a is the mean wind pressure which acts as a static load on the structure, and the response of mean wind pressure can be obtained by using a static method; P_d is the fluctuating wind pressure which acts as a dynamic load and induces random vibration of structure, and the response of the fluctuating wind pressure can be solved by using the methods of random vibration theory. In this paper, the response of beam under the dynamic load, the fluctuating wind pressure, is analyzed and controlled using the active actuators, so in the analyses hereafter only the fluctuating wind pressure is considered.
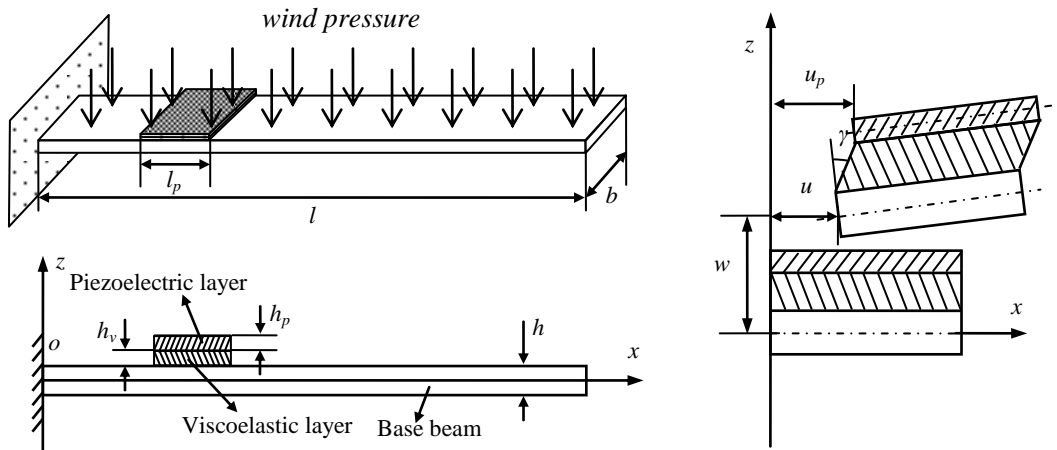

Fig. 1 The schematic diagrams of the beam and ACLD systems and the parameters under wind pressure

The following normalized power spectral density of the fluctuating wind speed has been proposed as Eq. (5) by Kaimal *et al.* (1972)

$$S_{v_d}(H,\omega) = v_*^2 \frac{200r_2}{\omega(1+50r_2)^{5/3}}, \quad r_2 = \frac{\omega H}{v_a(H)} \tag{5}$$

where ω is the frequency in Hz, the parameter v^* is the shear flow velocity which is determined by

$$v^* = \frac{k v_a(H)}{\ln(H/H_0)}$$ (6)

where k is von Karman's constant (generally assumed to be approximately 0.4), and H_0 is the roughness length (Simiu and Scalan (1986)), a variable characterizing the terrain.

From Eqs. (3) and (4) one can obtain the power spectral density of the fluctuating wind pressure

$$S_{P_d}(H, \omega) = \frac{4P_a^2}{v_a^2} S_{v_d}(H, \omega)$$ (7)

3. Analytical models

In Fig. 1 is shown the schematic diagrams of a cantilevered beam with an ACLD patch and their parameters. The ACLD patch is composed of a viscoelastic layer and a piezoelectric layer. As Fig. 1 shows, h, h_v and h_p are, respectively, the thicknesses of the base beam, the viscoelastic layer and the piezoelectric layer; l and l_p are the length of the base beam and the ACLD patch; and it is assumed that the ACLD patch has the same width b with the base beam. The axial and transverse displacements of the beam are set as u and w; the axial displacements of the piezoelectric layer is set as u_p; and the shear strain of the viscoelastic layer is set as γ.

Referencing from (Li 2008), the normal strain of the base beam ε_x, the normal strain of the piezoelectric layer ε_x^p and the shear strain of the viscoelastic layer γ can be written as

$$\varepsilon_x = \frac{\partial u}{\partial x} - z\frac{\partial^2 w}{\partial x^2}, \quad \varepsilon_x^p = \frac{\partial u_p}{\partial x} - z\frac{\partial^2 w}{\partial x^2}, \quad \gamma = \frac{u_p - u}{h_v} + \left(1 + \frac{h}{2h_v} + \frac{h_p}{2h_v}\right)\frac{\partial w}{\partial x}$$ (8)

With the modulus of elasticity c_{11} the normal stress of base beam can be written as

$$\sigma_x = c_{11}\varepsilon_x$$ (9)

For the ACLD system, the piezoelectric layer is assumed to be transversely isotropic and the polarization direction is in thickness direction. The constitutive equation of the piezoelectric layer is expressed as

$$\sigma_x^p = c_{11}^p\varepsilon_x^p - e_{31}E_z, \quad D_z = e_{31}\varepsilon_x^p + \in_{33}E_z$$ (10)

where σ_x^p is the normal stress, D_z and E_z are the electric displacement and the electric intensity in thickness direction, and c_{11}^p, e_{31} and $\in_{33}$ are the elastic constant, piezoelectric constant and dielectric constant of the piezoelectric layer. It is assumed that the electric field is uniform, so E_z can be expressed by the external voltage applied on the piezoelectric layer V_0 and the thickness h_p

$$E_z = -\frac{V_0}{h_p}$$ (11)

Another component of the ACLD treatment, namely the viscoelastic layer is assumed to be frequency dependent material with complex shear modulus $G_v = G_0(1 + i\eta_v)$ where G_0 and η_v are the storage shear modulus and loss factor which are dependent upon the vibration frequency, i denotes the imaginary symbol $\sqrt{-1}$.

The total kinetic energy T and potential energy U of beam/ACLD system can be written by

$$T_t = \frac{1}{2}\int_V \rho(\dot{u}^2 + \dot{w}^2)\mathrm{d}V + \frac{1}{2}\int_{V_p} \rho_p(\dot{u}_p^2 + \dot{w}^2)\mathrm{d}V + \frac{1}{2}\int_{V_v} \rho_v(\dot{u}^2 + \dot{w}^2)\mathrm{d}V \tag{12}$$

$$U_t = \frac{1}{2}\int_V \sigma_x\varepsilon_x\mathrm{d}V + \frac{1}{2}\int_{V_p} \sigma_x^p\varepsilon_x^p\mathrm{d}V - \frac{1}{2}\int_{V_p} D_z E_z\mathrm{d}V + \frac{1}{2}\int_{V_v} G_v\gamma^2\mathrm{d}V \tag{13}$$

where the dot denotes the differentiation with respect to time, ρ, ρ_p and ρ_v are the mass densities of the base beam, piezoelectric layer and viscoelastic layer; and V, V_p and V_v are the volumes of the base beam, piezoelectric layer and viscoelastic layer, respectively.

The work includes the works done by the fluctuating wind pressure and by the external applied electrical fields. The virtual work of the whole structural system can be written by

$$\delta W_t = \int_A P_\mathrm{d}\delta w\mathrm{d}A + \int_{A_p} D_z\delta V_0\mathrm{d}A \tag{14}$$

where $\delta(\cdot)$ denotes the first variation, A and A_p are the surface area of the base beam and the piezoelectric layer. In this analysis, it is assumed that the dimensions (l and b) of the beam is relatively small compared with the position (H) of the beam, so the fluctuating wind pressure in the surface areas of the beam is independent of l and b. In the other word, the fluctuating wind pressure in any point of the surface area A is a constant.

To use the Rayleigh-Ritz method, the displacements u, w and u_p should be expressed in terms of generalized coordinates

$$u(x,t) = \sum_{i=1}^n U_i(x)p_{ui}(t) = U^\mathrm{T}(x)p_u(t) \tag{15}$$

$$w(x,t) = \sum_{i=1}^n W_i(x)p_{wi}(t) = W^\mathrm{T}(x)p_w(t) \tag{16}$$

$$u_p(x,t) = \sum_{i=1}^n U_{pi}(x)p_{p_i}(t) = U_p^\mathrm{T}(x)p_p(t) \tag{17}$$

where $p_u(t) = [p_{ui},......,p_{un}(t)]^\mathrm{T}$, $p_w(t) = [p_{wi},......,p_{wn}(t)]^\mathrm{T}$ and $p_p(t) = [p_{pi},......,p_{pn}(t)]^\mathrm{T}$ are the generalized coordinates or modal coordinates of the structural system, and $U(x) = [U_1(x),......,U_n(x)]^\mathrm{T}$, $W(x) = [W_1(x),......,W_n(x)]^\mathrm{T}$ and $U_p(x) = [U_{p1}(x),......,U_{pn}(x)]^\mathrm{T}$ are the displacement shape functions or the principal vibration mode shapes which must satisfy the geometric boundary conditions.

Hamilton's principle is written by

$$\int_{t_1}^{t_2} \delta(T_t - U_t)\mathrm{d}t + \int_{t_1}^{t_2} \delta W_t \mathrm{d}t = 0 \tag{18}$$

Substituting Eqs. (8)-(17) into Eq. (18) and performing the variation operation in terms of $\boldsymbol{p}_u$, $\boldsymbol{p}_w$, $\boldsymbol{p}_p$ and V_0, the equations of motion of the whole system can be obtained

$$\boldsymbol{M}_t \ddot{\boldsymbol{p}} + \boldsymbol{K}_e V_0 + \boldsymbol{K}_t \boldsymbol{p} = \boldsymbol{f} P_d \tag{19}$$

where $\boldsymbol{M}_t$, $\boldsymbol{K}_e$, $\boldsymbol{K}_t$ and $\boldsymbol{f}$ are the generalized mass matrix, electromechanical coupling matrix, stiffness matrix, and forcing matrix of the whole system, respectively, and all of these matrices are listed in Appendix A. In Eq. (19) $\boldsymbol{p}$ is the arrangement of the generalized coordinates $\boldsymbol{p}_u$, $\boldsymbol{p}_w$, $\boldsymbol{p}_p$ as the following column matrix

$$\boldsymbol{p}(t) = [\boldsymbol{p}_u^T(t) \quad \boldsymbol{p}_w^T(t) \quad \boldsymbol{p}_p^T(t)]^{\mathrm{T}} \tag{20}$$

4. Active vibration control and analysis using random theory

Using appropriate external control voltage the piezoelectric constrained layer can be activated to obtain active damping and suppress structural vibration. Here, a negative velocity feedback control strategy is applied. The control voltage exerted to the piezoelectric actuator is proportional to the velocity at the position x_0. With this set the control voltage of the piezoelectric actuator can be expressed in terms of the transverse velocity at the position x_0 of the beam as

$$V_0(t) = -K\dot{w}(x_0, t) \tag{21}$$

where K is the feedback control gain for the piezoelectric actuator. By changing the value of K, we can get different results of structural vibration control.

Substituting Eq. (16) into Eq. (21), the control voltage can be written by

$$V_0(t) = -K\boldsymbol{W}^{\mathrm{T}}(x_0)\dot{\boldsymbol{p}}_w = -K\boldsymbol{K}_w \dot{\boldsymbol{p}}(t) \tag{22}$$

where the coefficient matrix $\boldsymbol{K}_w$ is written by

$$\boldsymbol{K}_w = [0 \quad \boldsymbol{W}^T(x_0) \quad 0] \tag{23}$$

Substituting Eq. (22) into Eq. (19), one can get the following equation of motion with active damping

$$\boldsymbol{M}_t \ddot{\boldsymbol{p}} + \boldsymbol{C}_t \dot{\boldsymbol{p}} + \boldsymbol{K}_t \boldsymbol{p} = \boldsymbol{f} P_d \tag{24}$$

where $\boldsymbol{C}_t$ is so called the active damping matrix due to the piezoelectric layer and is written by

$$\boldsymbol{C}_t = -K\boldsymbol{K}_e \boldsymbol{K}_w \tag{25}$$

It can be seen from Eq. (24) that the algorithm of negative velocity feedback control provides the active damping effect to control the structural vibration. In order to analyze the controlling properties of the active control of wind induced vibration, the dynamic Eq. (24) must be decoupled.

However, it can be seen from Eq. (25) that the matrix C_t is not symmetric. As a result, the equation of motion cannot be decoupled. Therefore, the complex modal analytical theory must be employed.

Defining the state vector $\boldsymbol{r} = [\boldsymbol{p}^T, \dot{\boldsymbol{p}}^T]^T$ and introducing this state vector into Eq. (24), one can obtain the state equation

$$\boldsymbol{A}\dot{\boldsymbol{r}} + \boldsymbol{B}\boldsymbol{r} = \boldsymbol{F}P_d \tag{26}$$

where $\boldsymbol{A}$, $\boldsymbol{B}$ and $\boldsymbol{F}$ are written as

$$\boldsymbol{A} = \begin{bmatrix} \boldsymbol{C}_t & \boldsymbol{M}_t \\ \boldsymbol{M}_t & \boldsymbol{0} \end{bmatrix}, \quad \boldsymbol{B} = \begin{bmatrix} \boldsymbol{K}_t & \boldsymbol{0} \\ \boldsymbol{0} & \boldsymbol{-M}_t \end{bmatrix}, \quad \boldsymbol{F} = \begin{Bmatrix} \boldsymbol{f} \\ \boldsymbol{0} \end{Bmatrix} \tag{27}$$

Solving the eigenvalue problem of Eq. (26), one can easily determine the system eigenvalue λ_i, and the left eigenvector $\boldsymbol{\Psi}_{Li}$, as well as the right eigenvector $\boldsymbol{\Psi}_{Ri}$ ($i = 1, 2 \ldots, 6n$).

Considered the orthogonality of the left and the right modal matrices, one has

$$-\lambda_i \boldsymbol{\Psi}_{Li}^T \boldsymbol{A} \boldsymbol{\Psi}_{Ri} = \boldsymbol{\Psi}_{Li}^T \boldsymbol{B} \boldsymbol{\Psi}_{Ri} = -\lambda_i J_i \,, \quad (i = 1, 2 \ldots, 6n) \tag{28}$$

where J_i is the complex norm quantity, then the decoupled dynamic equations of Eq. (26) can be expressed as

$$\dot{s}_i - \lambda_i s_i = \frac{1}{J_i} \boldsymbol{\Psi}_{Li}^T \boldsymbol{F}P_d \,, \quad (i = 1, 2 \ldots, 6n) \tag{29}$$

where s is the complex modal coordinate and one has the transform relationship

$$\boldsymbol{r} = \boldsymbol{\Psi}_R s \tag{30}$$

while $\boldsymbol{\Psi}_R$ is the matrix composed right eigenvectors, similarly, $\boldsymbol{\Psi}_L$ is the matrix composed left eigenvectors.

By Duhamel integration, the solution of Eq. (29) can be expressed as

$$s_i(t) = \frac{1}{J_i} \int_{-\infty}^{\infty} h_i(t - \tau) \boldsymbol{\Psi}_{Li}^T \boldsymbol{F}P_d(\tau) d\tau \,, \quad (i = 1, 2 \ldots, 6n) \tag{31}$$

where $h_i(t\text{-}\tau)$ is the impulse response function, the solution of Eq. (29) in the frequency domain can be written as

$$s_i(\omega) = \frac{1}{J_i} \int_{-\infty}^{\infty} \boldsymbol{\Psi}_{Li}^T \boldsymbol{F}P_d(\omega) H_i(\omega) e^{i\omega t} dt \,, \quad (i = 1, 2 \ldots, 6n) \tag{32}$$

where $H_i(\omega)$ is the ith modal complex frequency function and has the following form

$$H_i(\omega) = \int_{-\infty}^{\infty} h_i(t - \tau) e^{i\omega(t-\tau)} d\tau \,, \quad (i = 1, 2 \ldots, 6n) \tag{33}$$

With the transform relationship (30) $\boldsymbol{r}$ in the frequency and time domain can be obtained as

$$r(\omega) = \boldsymbol{\Psi}_R s(\omega) \ , \ r(t) = \boldsymbol{\Psi}_R s(t) \tag{34}$$

From Eqs. (16), (20) and (34), the transverse vibration responses w and vibration velocity $\dot{w}$ of the cantilevered beam in the frequency domain and time domain can be obtained

$$w(x,\omega) = \sum_{i=n+1}^{2n} \boldsymbol{W}_{i-n}(x)\boldsymbol{r}_i(\omega) \ , \ w(x,t) = \sum_{i=n+1}^{2n} \boldsymbol{W}_{i-n}(x)\boldsymbol{r}_i(t) \tag{35}$$

$$\dot{w}(x,\omega) = \sum_{i=4n+1}^{5n} \boldsymbol{W}_{i-4n}(x)\boldsymbol{r}_i(\omega) \ , \ \dot{w}(x,t) = \sum_{i=4n+1}^{5n} \boldsymbol{W}_{i-4n}(x)\boldsymbol{r}_i(t) \tag{36}$$

From expression (29) the cross-power spectrum of s can be obtained

$$S_{s,ij}(\omega) = H_i(\omega)\mu_i \boldsymbol{\Psi}_{Li}^T \boldsymbol{F} S_q(\omega) \boldsymbol{F}^T \boldsymbol{\Psi}_{Lj}\mu_j H_j^*(\omega) \ , (i, j = 1, 2 \ldots, 6n) \tag{37}$$

where $H_j^*(\omega)$ is the jth modal conjugate complex frequency function. By further considering the expression of the model transformation (30), the response power spectrum matrix $S_r(\omega)$ in state space can be expressed as

$$[S_r(\omega)] = \boldsymbol{\Psi}_R [S_s(\omega)] \boldsymbol{\Psi}_R^T \tag{38}$$

where $S_s(\omega)$ is the power spectrum matrix composed by elements $S_{s,ij}$.

Finally, the mean-square value of the transverse vibration responses and vibration velocity of the cantilevered beam can be obtained

$$E[w(x)^2] = \sum_{i=n+1}^{2n} \sum_{j=n+1}^{2n} \boldsymbol{W}_{i-n}(x)\boldsymbol{W}_{i-n}(x)S_{r,ij}(\omega) \tag{39}$$

$$E[\dot{w}(x)^2] = \sum_{i=4n+1}^{5n} \sum_{j=4n+1}^{5n} \boldsymbol{W}_{i-4n}(x)\boldsymbol{W}_{j-4n}(x)S_{r,ij}(\omega) \tag{40}$$

In order to solve Eq. (26), one must present the formulations of the principal mode shapes $\boldsymbol{U}(x)$, $\boldsymbol{W}(x)$ and $\boldsymbol{U}_p(x)$ in Eqs. (15)-(17). According to the theory of structural dynamics, the mode shapes for the longitudinal and transverse displacements of the cantilevered beam can be expressed as

$$\boldsymbol{U}_i(x) = \sin \mu_i x \ , \ \ \mu_i = \frac{(2i-1)\pi}{2l} \ , (i, j = 1, 2 \ldots, 6n) \tag{41}$$

$$\boldsymbol{W}_i(x) = \cosh \gamma_i x - \cos \gamma_i x - \frac{\cosh \gamma_i l + \cos \gamma_i l}{\sinh \gamma_i l + \sin \gamma_i l}(\sinh \gamma_i x - \sin \gamma_i x) \ , (i, j = 1, 2 \ldots, 6n) \tag{42}$$

where γ_i is determined by

$$\cos \gamma_i l \cosh \gamma_i l + 1 = 0 \ , (i, j = 1, 2 \ldots, 6n) \tag{43}$$

The axial mode shape $\boldsymbol{U}_{pi}$ for the piezoelectric constrained layer is modeled as the longitudinal vibration mode shape of the rod with free-free boundaries. It can be given by

$$\boldsymbol{U}_{pi}(x) = \cos\upsilon_i x\,, \quad \upsilon_i = \frac{i\pi}{l_p}\,, \quad (i, j = 1, 2\ldots, 6n) \tag{44}$$

In this study, the first five vibration mode shapes are considered, i.e. n equals to 5.

5. Numerical simulations and discussions

In this section, the performance of active treatments is studied for suppressing wind induced vibration of the cantilevered beams. The base beam is aluminum and the active piezoelectric constrained layer is PZT-4. The chosen structure and material parameters are taken as following

(a) c_{11}= 70.0 GPa, ρ=2710 Kg/m^2, l = 1.0m, b = 0.1 m and h = 0.01 m

(b) c_{11}^p= 64.5 GPa, e_{31}=-5.203 C/m^2, ρ_p=7500 Kg/m^2, l_p = 0.2 m, h_p = 0.0005 m

(c) ρ_v = 750 kg/m^3, v_v=0.499, h_v = 0.0005 m

The Young's modulus and the loss factor of the viscoelastic material referenced from (Li and Narita 2012b, 2013a) are given by

$$\log[2(1+v_v)G_v] = 0.106\log\omega + 1.52, \quad G_v(\text{MPa}) \tag{45}$$

$$\eta_v = 39.4 - 5.56\log\omega, \quad \eta_v\,(\%) \tag{46}$$

5.1 Analysis of the natural frequencies

The natural frequencies of the cantilevered base beam without ACLD patch have been calculated by presenting analysis and comparing with the results obtained by dynamics theory. Using the dynamics theory the formula of the first five frequencies can be written as

$$\omega_1 = 1.875^2 D\,, \quad \omega_2 = 4.694^2 D\,, \quad \omega_3 = 7.855^2 D\,, \quad \omega_4 = (3.5\pi)^2 D\,, \omega_5 = (4.5\pi)^2 D \tag{47}$$

where $D = \sqrt{EJ/4\pi^2 ml^3}$ and J is the area moment of inertia of the base beam and m is the mass of the beam. The results are listed as follow:

Present analysis: 8.2100 Hz, 51.4514 Hz, 144.0653 Hz, 282.3105 Hz, 466.6795 Hz
Dynamics theory: 8.2091 Hz, 51.4494 Hz, 144.0742 Hz, 282.3122 Hz, 466.6794 Hz

It is seen that the results of the present approach are in excellent agreement with the results of the dynamics theory and the validity of the analytical method is established.

5.2. Active control of wind pressure

For different control gains, the transverse responses at the top of the beam in the time domain and frequency domain are investigated. The velocity sensor is on the top of the beam and its position coordinate is x_0 = 1.0 m. It has been found that an ACLD patch placed close to the fixed end is more effective in controlling the vibration of beam (Li *et al.* 2003). In this study the ACLD patch is bonded at x_1 = 0.2 m and x_2 = 0.4 m of the beam.

Noticed that the wind pressure as random dynamic load can be considered as consisting of a series of pulses, firstly, the response at the top of the beam is investigated under a Gaussian

impulse (the amplitude of the Gaussian pulse is 1 N/m^2) which simulates a fluctuating wind pressure pulse acting as a dynamic load. Figs. 2 and 3 illustrate the response and velocity at the top of the beam in the time domain with the control gain $K = 0$, 1.5×10^4 and 3.0×10^4. From Figs. 2 and 3 one can observe that with the increase of control gain K the amplitudes of the displacement and velocity reduce seriously. This shows that the ACLD patch can significantly improve the damping characteristics of the beam and the vibration can be suppressed effectively. Fig. 4 shows the active control voltages corresponding to Fig. 2. It is seen from this numerical result that with a much smaller control voltage (only 30 V) one can achieve a significantly attenuation of the vibration.
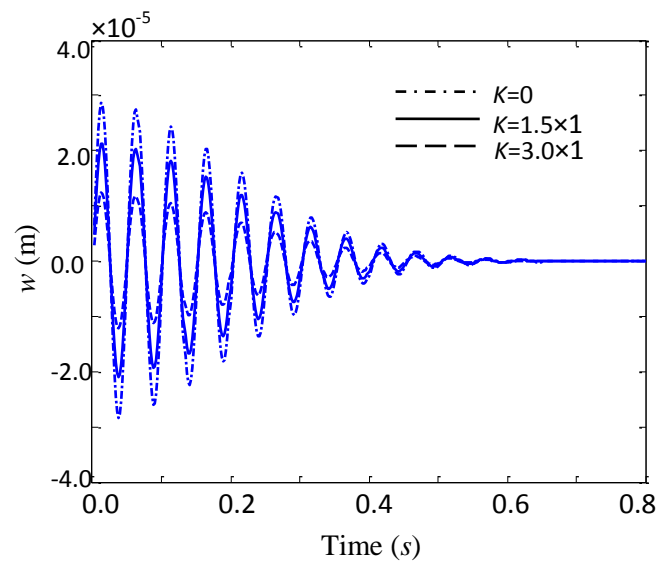
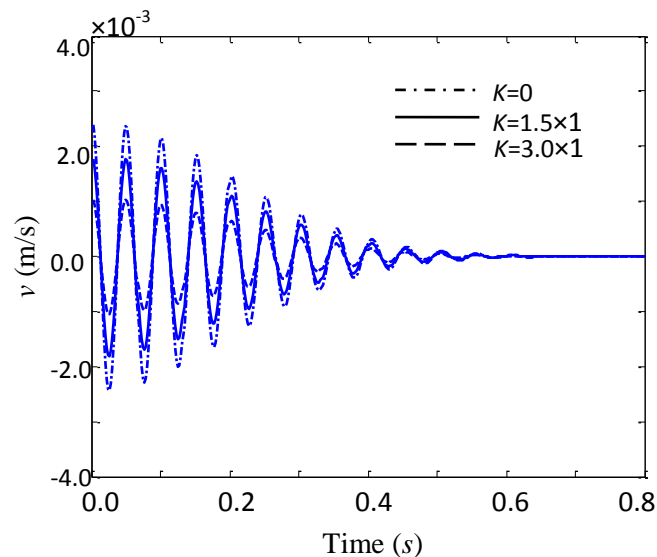Fig. 2 Displacement vs. time under different control gain K

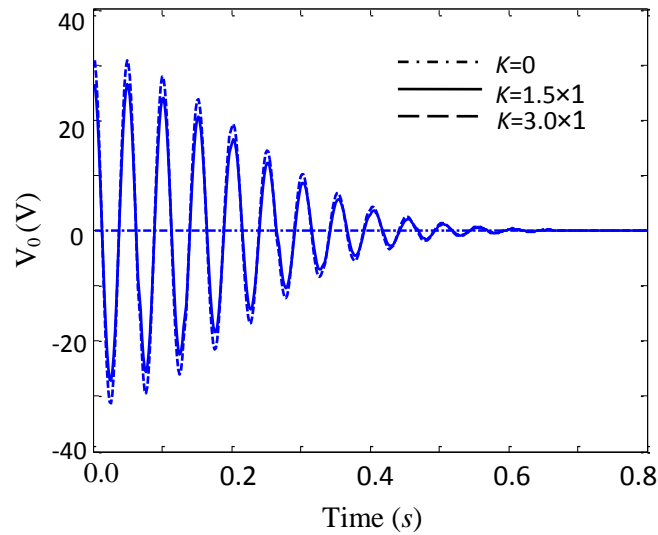Fig. 3 Velocity vs. time under different control gain K

Fig. 4 Voltage vs. time under different control gain *K*

Figs. 5, 6 and 7 show the uncontrolled and controlled frequency responses at the top of the beam, the same active damping effects are obtained. And it is found that for different control gain the maximum control voltage for every resonant response is almost the same especially for the first and second one.
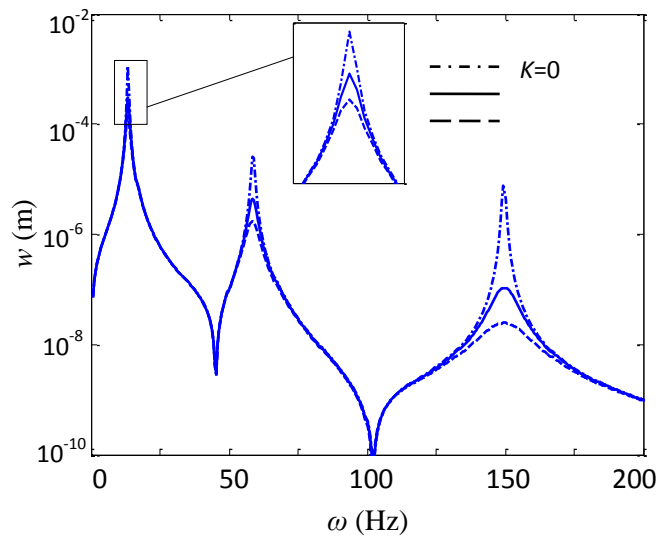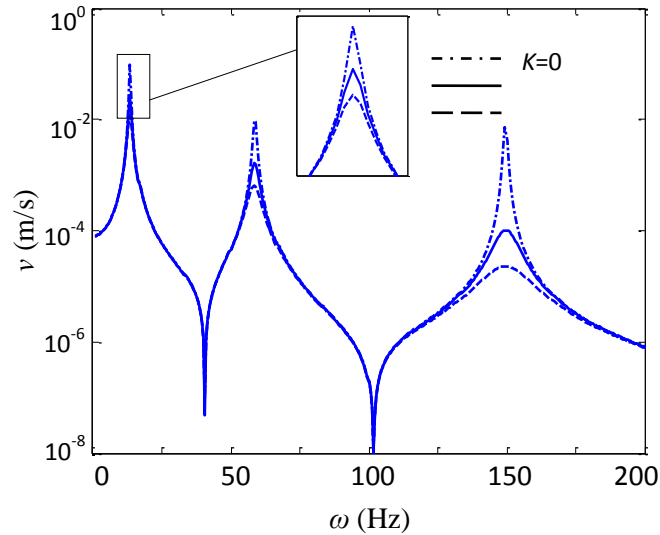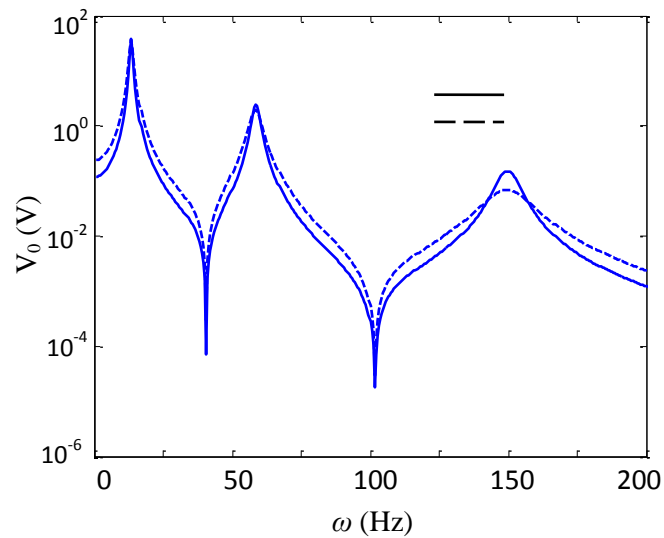

Fig. 5 Displacement vs. frequency under different *K*

Fig. 6 Velocity vs. frequency under different *K*

Fig. 7 Voltage vs. frequency under different *K*

To investigate the effects of active constrained layer on the vibration control of a cantilevered beam under wind pressure, the power spectrum and mean-squares displacements are simulated under different control gains. To use the velocity conversion of Eqs. (4) and (5), the terrain is regarded as the city centre with high- and low-rise buildings where the roughness length is taken to be H_0=2.0 (Wieringa 1998). The height of the beam is assumed to be H=10 m and the mean wind speed at this height is $v_a(10)$=8 m/s (Moderate breeze). Using Kaimal wind velocity conversion, at the top of the cantilevered beam the power spectrum curves of response and velocity, with and without active control, are drawn up and shown in Fig. 8. It can be found that the peak value of

spectral density at a low natural frequency is much larger than at a high natural frequency. That is to say the mean-square value of the transverse displacement is mainly decided by the first few vibration modes especially the first one which corresponding the lowest natural frequency. Because the random vibration power is mainly distributed in the low frequency band, the vibration suppression for the first few vibration modes is very important. From these figures, one can find that, with increasing feedback gain, the peak values of power spectral density of the first three modes attenuate significantly.
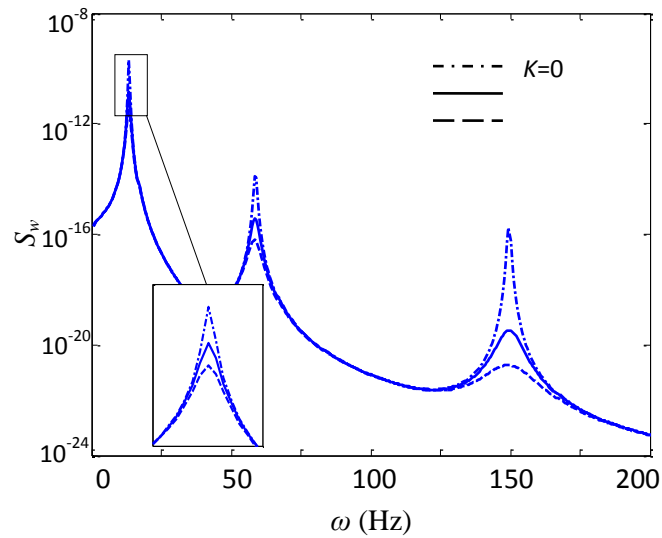

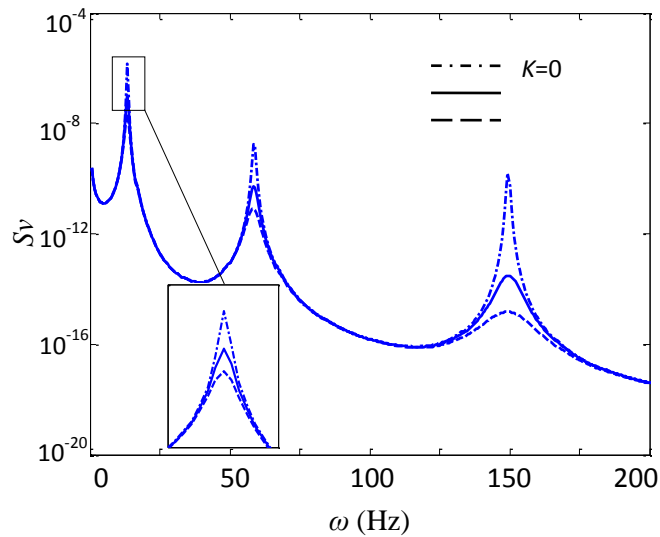Fig. 8 Spectral density of displacement vs. frequency

Fig. 9 Spectral density of velocity vs. frequency

To study the influences of the control gain on the wind induced vibration, the Mean-squares displacements and velocity under different control gains are studied. From Figs. 10 and 11 one can find that with the increase of control gain K the amplitudes of the displacement and velocity reduce seriously. And with the increase of control gain the descent rate of Mean-squares values (the slopes of curves in the figures) decrease. From these figures one also finds that the cantilevered beam position significantly affects the values of Mean-squares displacements and velocity, it will be further studied in the next section.
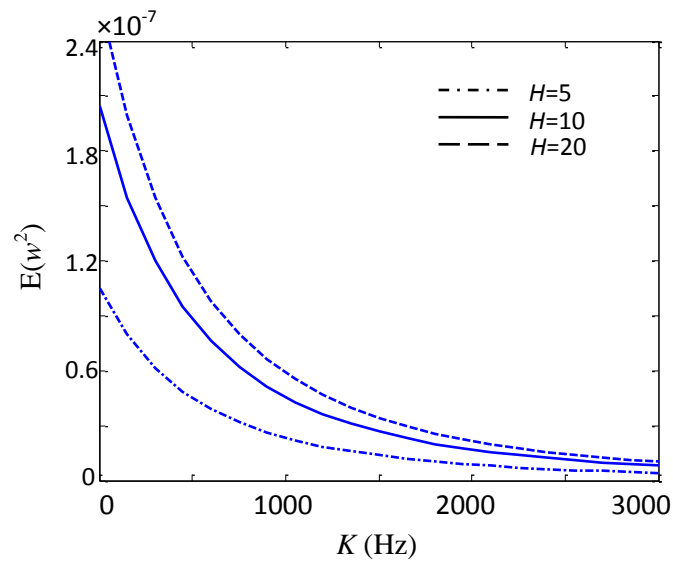

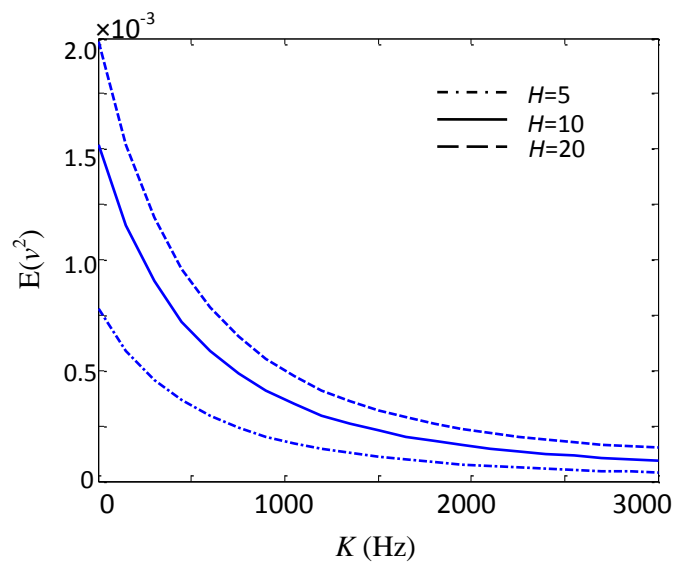Fig. 10 Mean-squares displacement vs. control gain K

Fig. 11 Mean-squares velocity vs. control gain K
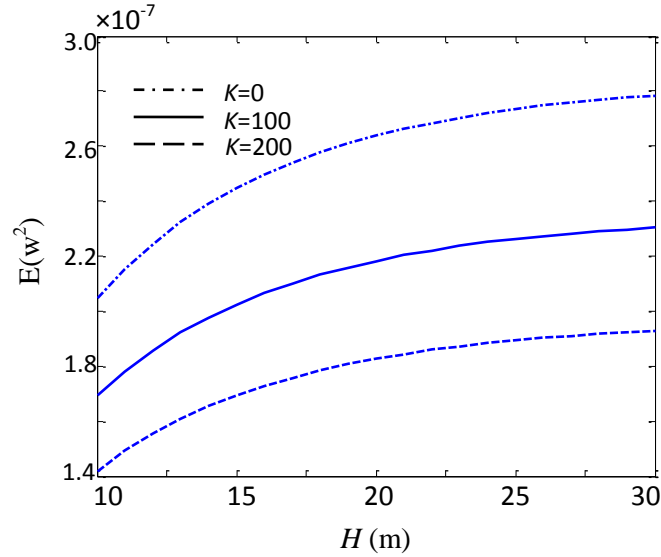
Fig. 12 Mean-squares displacement vs. the height of beam

Using Kaimal wind velocity conversion, the mean-squares displacements and velocity vs. *H* are illustrated in Figs. 12 and 13. From these figures one can find that the mean-squares displacements and velocity are strongly influenced by the height of beams. And when the height increases to a certain value (here it is about 20 m), its effect becomes limited. Also it can be found from these curves that with increasing feedback gain, the mean-squares displacements under wind pressure attenuate significantly, this clearly shows that this method can effectively reduce the vibration caused by wind pressure.

Fig. 13 Mean-squares velocity vs. the height of beam

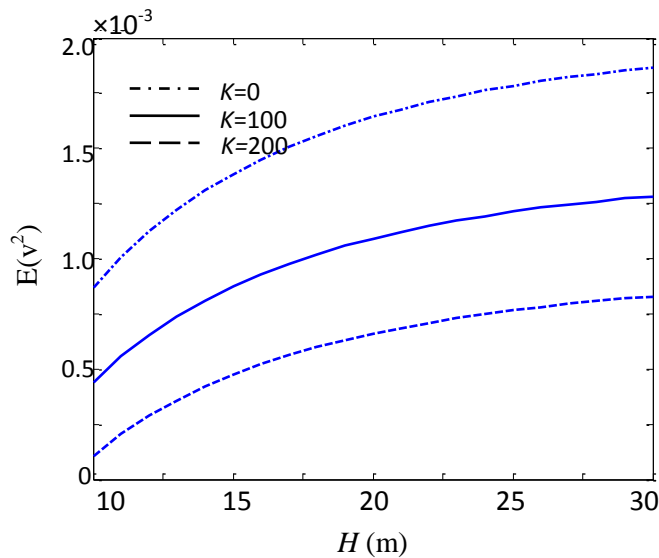## 6. Conclusions

The present paper is devoted to the analysis of active control of the wind induced vibration with ACLD patch. The equation of motion is derived by Rayleigh-Ritz method and random vibration theory. The active vibration control of beam under wind pressure is analytically investigated. It is seen from the numerical results that using a negative velocity feedback control strategy the active damping is obtained and the amplitudes of the wind induced vibration can be efficiently attenuated with much smaller control voltages. The analytical methodology can be expanded to other kinds of random vibration such as earthquake induced vibration and water flow induced vibration.

References

Balamurugan, V. and Narayanan, S. (2002), "Active–passive hybrid damping in beams with enhanced smart constrained layer treatment", *Eng. Struct.*, **24**, 355-363.

Cai, C., Zheng, H., Hung, K.C. and Zhang, Z.J. (2006), "Vibration analysis of a beam with an active constraining layer damping patch", *Smart Mater. Struct.*, **15**, 147-156.

Chai, W. and Feng, M.Q. (1997), "Vibration control of super tall buildings subjected to wind loads", *Int. J. Nonlinear Mech.*, **32**(4), 657-668.

Kaimal, J.C.,Wyngaard, J.C., Izumi, Y. and Coté, O.R. (1972), "Spectral characteristics of surface-layer, Turbulence", *Q. J. Roy. Meteor. Soc.*, **98**, 563-589.

Kolousek, V., Pirner, M., Fischer, O. and Naprstek, J. (1984), *Wind effects on civil engineering structures*, Elsevier, Amsterdam.

Kubo, Y., Modi, V.J., Kotsubo, C., Hayashida, K. and Kato, K. (1996), "Suppression of wind-induced vibrations of tall structures through moving surface boundary-layer control", *J. Wind Eng. Ind. Aerod.*, **61**, 181-194.

Kwok, K.C.S. and Samali, B. (1995), "Performance of tuned mass dampers under wind loads", *Eng. Struct.*, **17**(9) , 655-667.

Lee, J.T. (2005), "Active structural acoustics control of beams using active constrained layer damping through loss factor maximization", *J. Sound Vib.*, **287**, 481-503.

Lee, U. and Kim, J. (2001), "Spectral element modeling for the beams treated with active constrained layer damping", *Int. J. Solids Struct.*, **38**, 5679-5702.

Li, F.M., Kishimoto, K., Wang, Y.S., Chen, Z.B. and Huang, W.H. (2008), "Vibration control of beams with active constrained layer damping", *Smart Mater. Struct.*, **17**, 1-9.

Li, F.M. (2012) "Active aeroelastic flutter suppression of a supersonic plate with piezoelectric material", *Int. J. Eng. Sci.*, **51**, 190-203.

Li, J. and Narita, Y. (2012a), "Vibration suppression for laminated cylindrical panels with arbitrary edge conditions", *J. Vib. Control*, **19**(4), 626-640.

Li, J. and Narita, Y. (2012b), "The effect of aspect ratios and edge conditions on optimal damping design of thin soft core sandwich plates and beams", *J. Vib. Control*, DOI: 10.1177/1077546312463756.

Li, J. and Narita, Y. (2013a), "Analysis and optimal design for the damping property of laminated viscoelastic plates under general edge conditions", Composites Part B, 45, 972-980.

Li, J. and Narita, Y. (2013b), "Analysis and optimal design for supersonic composite laminated plate", *Compos. Struct.*, **101**, 35-46.

Simiu, F. and Scanlan, R.H. (1986), *Wind effects on structures*, 2nd Ed., Wiley, New York.

Solari, G. (1997), "Wind excited response of structures with uncertain parameters", *Probabilist. Eng. Mech.*, **12**(2), 75-87.

Sun, D. and Tong, L. (2004), "A compressional-shear model for vibration control of beams with active constrained layer damping", *Int. J. Mech. Sci.*, **46**, 1307-1325.

Vasques, C.M.A., Mace, B.R., Gardonio, P. and Rodrigues, J.D. (2006), "Arbitrary active constrained layer damping treatments on beams, finite element modelling and experimental validation", *Comput. Struct.*, **84**, 1384-1401.

Wieringa, J. (1998), "How far can agrometeorological station observations be considered representative", *Proceedings of the 23rd Conference on Agricul- tural and Forest Meteorology*, 2-6 November (N. Mex., USA). Weather data requirements for Integrated Pest Management, 9-12. American Meteorological Society.

Zhang, J. and Roschke, P.N. (1999), "Active control of a tall structure excited by wind", *J. Wind Eng. Ind. Aerod.*, **83**, 209-223.

CC

Appendix A

The expressions of the modal mass, modal stiffness and forcing matrices in Eq. (19) are given

$$\boldsymbol{M}_t = \begin{bmatrix} \boldsymbol{M}_{b1} + \boldsymbol{M}_{v1} & 0 & 0 \\ 0 & \boldsymbol{M}_{b2} + \boldsymbol{M}_{p2} + \boldsymbol{M}_{v2} & 0 \\ 0 & 0 & \boldsymbol{M}_{p1} \end{bmatrix},$$

$$\boldsymbol{K}_t = \begin{bmatrix} \boldsymbol{K}_{b1} + \boldsymbol{K}_{v1} & \boldsymbol{K}_{v4} & \boldsymbol{K}_{v3} \\ \boldsymbol{K}_{v4}^{\mathrm{T}} & \boldsymbol{K}_{b2} + \boldsymbol{K}_{p3} + \boldsymbol{K}_{v6} & \boldsymbol{K}_{p2}^{\mathrm{T}} + \boldsymbol{K}_{v5}^{\mathrm{T}} \\ \boldsymbol{K}_{v3}^{\mathrm{T}} & \boldsymbol{K}_{p2} + \boldsymbol{K}_{v5} & \boldsymbol{K}_{p1} + \boldsymbol{K}_{v2} \end{bmatrix},$$

$$\boldsymbol{K}_e = [0 \quad \boldsymbol{K}_{p5} \quad \boldsymbol{K}_{p4}]^{\mathrm{T}}, \quad \boldsymbol{f} = [0 \quad \boldsymbol{F}_q \quad 0]^{\mathrm{T}},$$

$$\boldsymbol{M}_{b1} = \rho b h \int_0^l \boldsymbol{U}(x)\boldsymbol{U}^{\mathrm{T}}(x)\mathrm{d}x, \quad \boldsymbol{M}_{b2} = \rho b h \int_0^l \boldsymbol{W}(x)\boldsymbol{W}^{\mathrm{T}}(x)\mathrm{d}x,$$

$$\boldsymbol{M}_{p1} = \rho_p b h_p \int_{x_1}^{x_2} \boldsymbol{U}_p(x)\boldsymbol{U}_p^{\mathrm{T}}(x)\mathrm{d}x, \quad \boldsymbol{M}_{p2} = \rho_p b h_p \int_{x_1}^{x_2} \boldsymbol{W}(x)\boldsymbol{W}^{\mathrm{T}}(x)\mathrm{d}x,$$

$$\boldsymbol{M}_{v1} = \rho_v b h_v \int_{x_1}^{x_2} \boldsymbol{U}(x)\boldsymbol{U}^{\mathrm{T}}(x)\mathrm{d}x, \quad \boldsymbol{M}_{v2} = \rho_v b h_v \int_{x_1}^{x_2} \boldsymbol{W}(x)\boldsymbol{W}^{\mathrm{T}}(x)\mathrm{d}x,$$

$$\boldsymbol{K}_{b1} = Ebh \int_0^l \frac{\mathrm{d}\boldsymbol{U}(x)}{\mathrm{d}x} \frac{\mathrm{d}\boldsymbol{U}^{\mathrm{T}}(x)}{\mathrm{d}x}\mathrm{d}x, \quad \boldsymbol{K}_{b2} = \frac{Ebh^3}{12} \int_0^l \frac{\mathrm{d}^2\boldsymbol{W}(x)}{\mathrm{d}x^2} \frac{\mathrm{d}^2\boldsymbol{W}^{\mathrm{T}}(x)}{\mathrm{d}x^2}\mathrm{d}x,$$

$$\boldsymbol{K}_{p1} = c_{11} b h_p \int_{x_1}^{x_2} \frac{\mathrm{d}\boldsymbol{U}_p(x)}{\mathrm{d}x} \frac{\mathrm{d}\boldsymbol{U}_p^{\mathrm{T}}(x)}{\mathrm{d}x}\mathrm{d}x,$$

$$\boldsymbol{K}_{p2} = -\frac{c_{11}b}{2}\left[\left(\frac{h}{2}+h_v+h_p\right)^2 - \left(\frac{h}{2}+h_v\right)^2\right]\int_{x_1}^{x_2} \frac{\mathrm{d}\boldsymbol{U}_p(x)}{\mathrm{d}x} \frac{\mathrm{d}^2\boldsymbol{W}^{\mathrm{T}}(x)}{\mathrm{d}x^2}\mathrm{d}x,$$

$$\boldsymbol{K}_{p3} = \frac{c_{11}b}{3}\left[\left(\frac{h}{2}+h_v+h_p\right)^3 - \left(\frac{h}{2}+h_v\right)^3\right]\int_{x_1}^{x_2} \frac{\mathrm{d}^2\boldsymbol{W}(x)}{\mathrm{d}x^2} \frac{\mathrm{d}^2\boldsymbol{W}^{\mathrm{T}}(x)}{\mathrm{d}x^2}\mathrm{d}x,$$

$$\boldsymbol{K}_{p4} = -e_{31}b \int_{x_1}^{x_2} \frac{\mathrm{d}\boldsymbol{U}_p^{\mathrm{T}}(x)}{\mathrm{d}x}\mathrm{d}x, \quad \boldsymbol{K}_{p5} = \frac{be_{31}}{2h_p}\left[\left(\frac{h}{2}+h_v+h_p\right)^2 - \left(\frac{h}{2}+h_v\right)^2\right]\int_{x_1}^{x_2} \frac{\mathrm{d}^2\boldsymbol{W}^{\mathrm{T}}(x)}{\mathrm{d}x^2}\mathrm{d}x,$$

$$\boldsymbol{K}_{p6} = -\frac{b \in_{33}}{h_p}(x_2 - x_1), \quad \boldsymbol{K}_{v1} = \frac{G_v b}{h_v}\int_{x_1}^{x_2}\boldsymbol{U}(x)\boldsymbol{U}^{\mathrm{T}}(x)\mathrm{d}x,$$

$$\boldsymbol{K}_{v2} = \frac{G_v b}{h_v}\int_{x_1}^{x_2}\boldsymbol{U}_p(x)\boldsymbol{U}_p^{\mathrm{T}}(x)\mathrm{d}x, \quad \boldsymbol{K}_{v3} = -\frac{G_v b}{h_v}\int_{x_1}^{x_2}\boldsymbol{U}(x)\boldsymbol{U}_p^{\mathrm{T}}(x)\mathrm{d}x,$$

$$\boldsymbol{K}_{v4} = -G_v b\left(1+\frac{h}{2h_v}+\frac{h_p}{2h_v}\right)\int_{x_1}^{x_2}\boldsymbol{U}(x)\frac{\mathrm{d}\boldsymbol{W}^{\mathrm{T}}(x)}{\mathrm{d}x}\mathrm{d}x,$$

$$\boldsymbol{K}_{v5} = G_v b\left(1+\frac{h}{2h_v}+\frac{h_p}{2h_v}\right)\int_{x_1}^{x_2}\boldsymbol{U}_p(x)\frac{\mathrm{d}\boldsymbol{W}^{\mathrm{T}}(x)}{\mathrm{d}x}\mathrm{d}x,$$

$$\boldsymbol{K}_{v6} = G'bh_v\left(1+\frac{h}{2h_v}+\frac{h_p}{2h_v}\right)^2\int_{x_1}^{x_2}\frac{\mathrm{d}\boldsymbol{W}(x)}{\mathrm{d}x}\frac{\mathrm{d}\boldsymbol{W}^{\mathrm{T}}(x)}{\mathrm{d}x}\mathrm{d}x,$$

$$\boldsymbol{F}_q = b\int_0^l\boldsymbol{W}^{\mathrm{T}}(x)\mathrm{d}x, \quad \boldsymbol{F}_{p1} = be_{31}\int_{x_1}^{x_2}\frac{\mathrm{d}\boldsymbol{U}_p^{\mathrm{T}}(x)}{\mathrm{d}x}\mathrm{d}x,$$

$$\boldsymbol{F}_{p2} = -be_{31}\left(\frac{h}{2}+h_v+h_p\right)\int_{x_1}^{x_2}\frac{\mathrm{d}^2\boldsymbol{W}^{\mathrm{T}}(x)}{\mathrm{d}x^2}\mathrm{d}x.$$